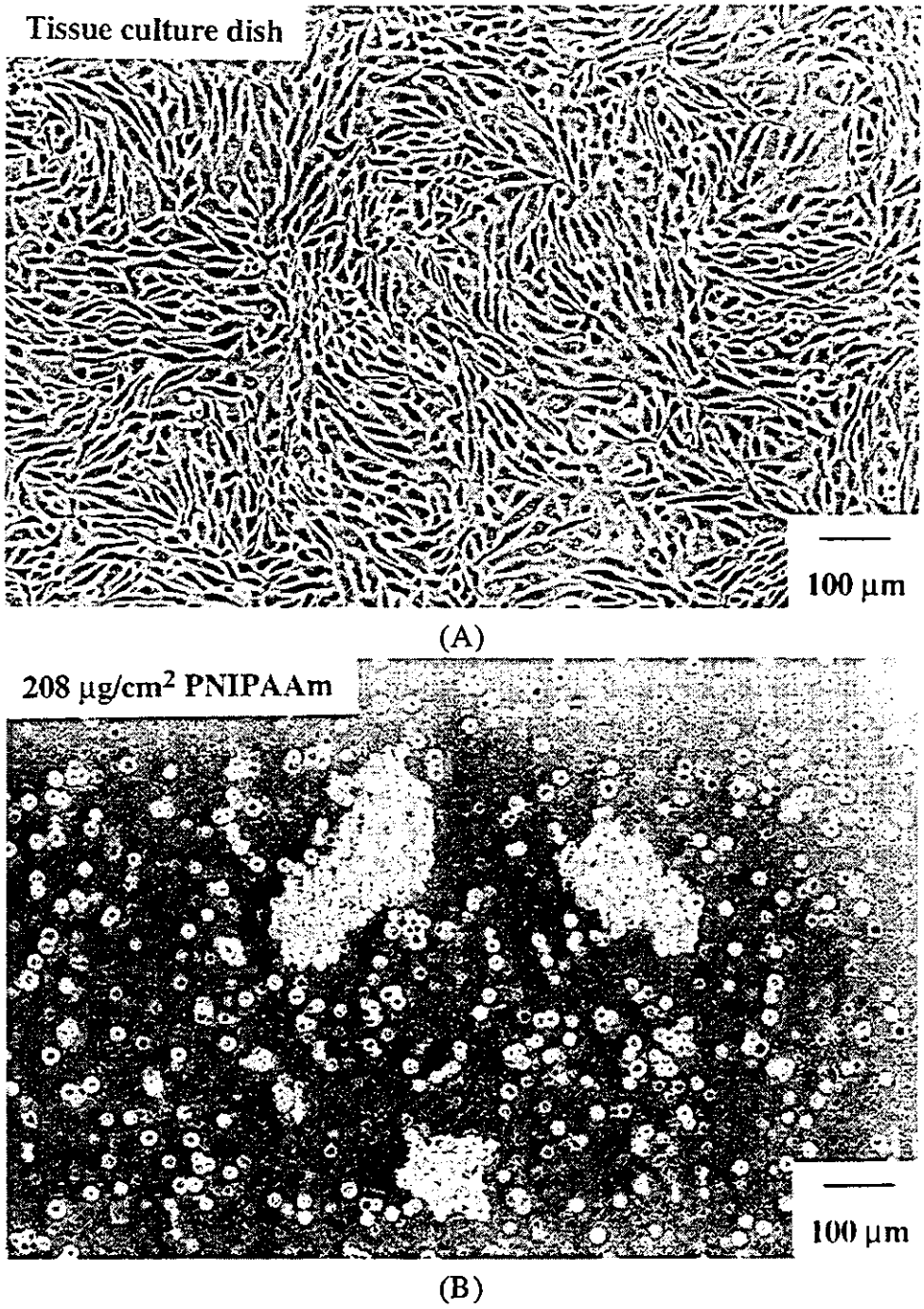

Figure 2. Phase-contrast micrographs of ECs cultured on (A) tissue culture dish, (B) dish coated with PNIPAAm (208 $\mu g/cm^2$), (C) dish coated with a mixture of gelatin (20.8 $\mu g/cm^2$) and PNIPAAm (208 $\mu g/cm^2$), and (D) dish coated with PNIPAAm-grafted gelatin (83.2 $\mu g/cm^2$). Surface area of dishes is 9.62 cm^2.

day. Then, the dishes were allowed to stand at 20°C. When ECs were cultured on dishes coated with only PNIPAAm (208 $\mu g/cm^2$), cells neither adhered nor spread; rather, they tended to aggregate with incubation time (Fig. 2B). Gelatin coating induced cell adhesion and spreading similarly to tissue culture dishes (Fig. 2A) but,

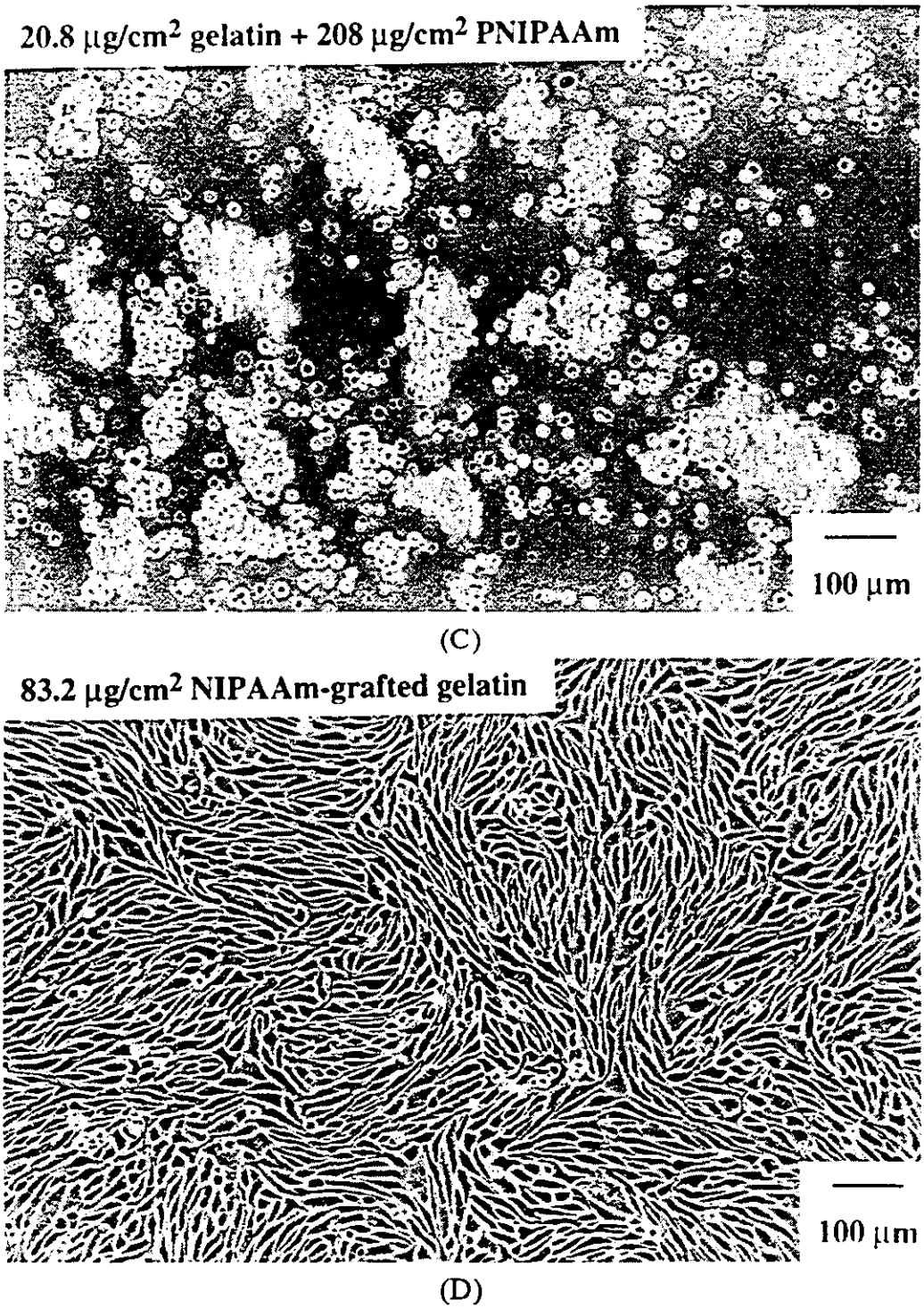

Figure 2. (Continued).

as expected, little delamination occurred at 20°C. On the other hand, the mixed coating of gelatin (20.8 $\mu g/cm^2$) and PNIPAAm (20.8 $\mu g/cm^2$) did not induce cell adhesion (Fig. 2C), whereas coating of PNIPAAm-gelatin (83.2 $\mu g/cm^2$) induced cell adhesion and spreading (Fig. 2D). However, standing at 20°C did not

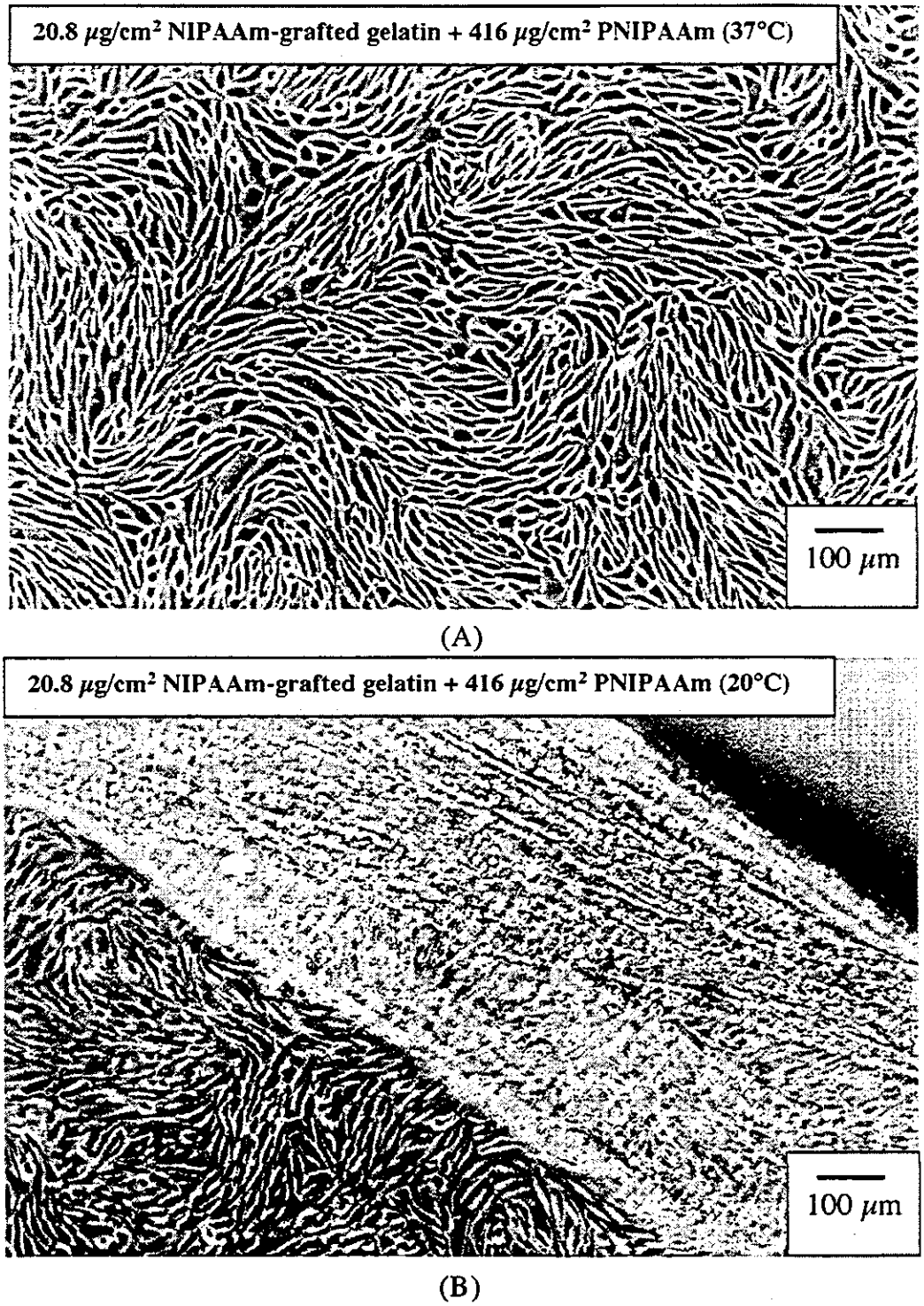

Figure 3. Phase-contrast micrographs of ECs cultured on (A and B) dish coated with a mixture of PNIPAAm-grafted gelatin (20.8 $\mu g/cm^2$) and PNIPAAm (416 $\mu g/cm^2$), (C) dish coated with a mixture of PNIPAAm-grafted gelatin (4.16 $\mu g/cm^2$) and PNIPAAm (208 $\mu g/cm^2$), and (D) dish coated with a mixture of PNIPAAm-grafted gelatin (4.16 $\mu g/cm^2$) and PNIPAAm (416 $\mu g/cm^2$). Surface area of dishes is 9.62 cm^2. (A) Confluent monolayer cultured at 37°C and (B) commencement of detachment by reducing temperature below LCST (20°C).

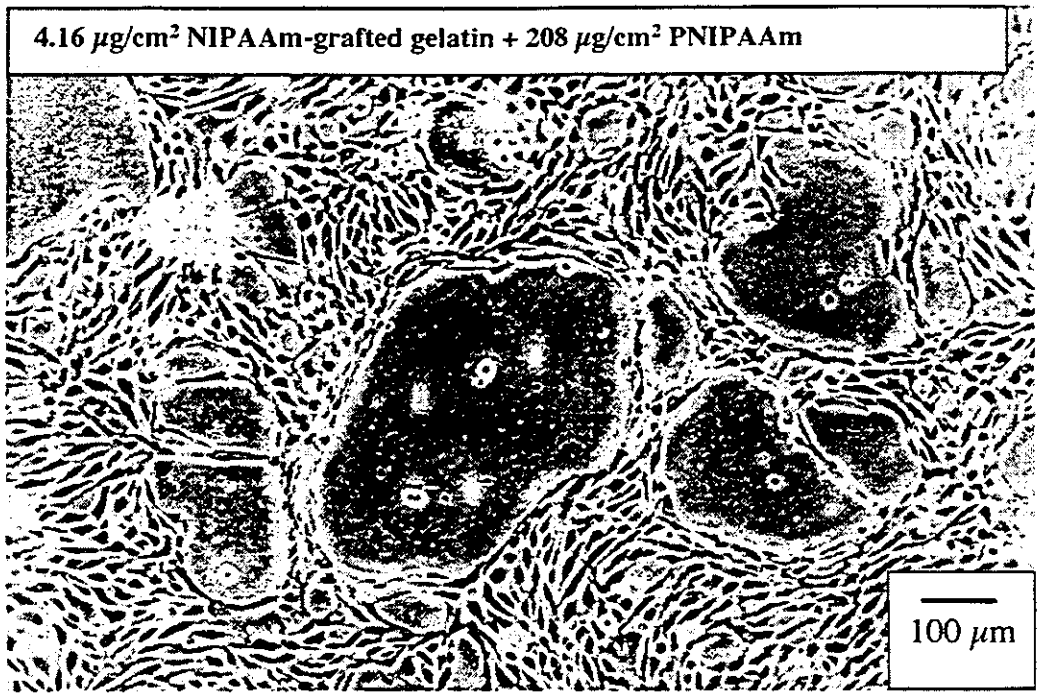

(C)

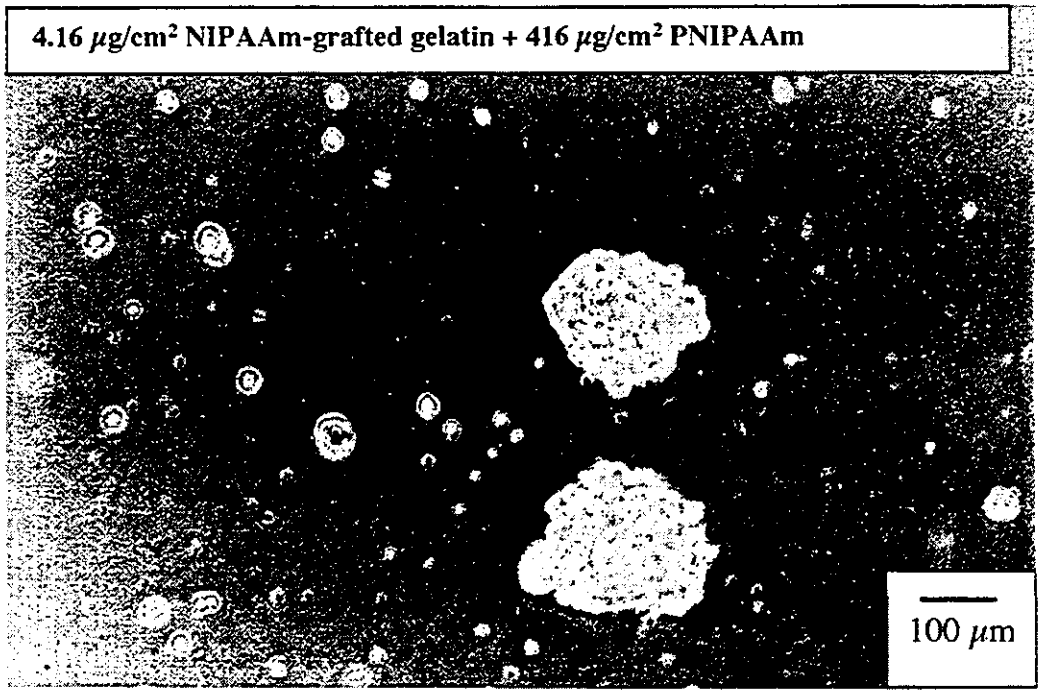

(D)

Figure 3. (Continued).

induce complete cell sheet detachment: only approximately 10% of the cells were detached. A monolayer sheet was obtained after incubation for one day. When the ambient temperature was decreased to 20°C, the sheet of monolayered cells was partially delaminated.

It is of interest to determine whether or not a mixture of PNIPAAm-gelatin and PNIPAAm induces monolayer sheet formation at 37°C and complete sheet delamination at 20°C. To this end, the effect of varying the ratio of these two components was examined (at two concentrations with respect to each other). The concentration of PNIPAAm-gelatin was fixed at 4.16 or 20.8 $\mu g/cm^2$ and that of PNIPAAm was fixed at 208 or 416 $\mu g/cm^2$. Thus, four combinations of concentrations were tested as follows. At first, PNIPAAm-gelatin concentration was fixed at 20.8 $\mu g/cm^2$. For the case of coating (gelatin content in the mixture: 1.43 wt%) with a mixture of this and with PNIPAAm (416 $\mu g/cm^2$), cells were found to adhere and spread well (Fig. 3A). At 20°C, the sheet of cells started to detach itself from the dish within several minutes (Fig. 3B), and after standing for approximately 20 min the cell sheet was completely detached and was floating on the medium. The coating (gelatin content in the mixture: 2.85% wt%) with a mixture of this with PNIPAAm (208 $\mu g/cm^2$) induced cell adhesion, but the percentage of cell adhesion was approximately 80% of that on the tissue culture dish and the percentage detachment of cells upon standing at room temperature was approximately 75% of the adhered cells. Cells did not completely detach from the dish at 20°C. On the other hand, at a low concentration of PNIPAAm-grafted gelatin (4.16 $\mu g/cm^2$), coating (gelatin content in the mixture: 0.58%) with a mixture of this and PNIPAAm (208 $\mu g/cm^2$) exhibited lower cell adhesion than that on the control tissue culture dish (Fig. 3C). On the other hand, no cell attachment was observed on dishes coated with a mixture with PNIPAAm (416 $\mu g/cm^2$) (Fig. 3D). These results are summarized in Fig. 4. The surface coated with a mixture of PNIPAAm-gelatin (20.8 $\mu g/cm^2$) and PNIPAAm (416 $\mu g/cm^2$) provided cell behaviors cell behaviors with complete cell adhesion and detachment.

DISCUSSION

The unique feature of the thermoresponsive phase transition of PNIPAAm has been utilized to develop 'intelligent' or 'smart' matrices for biomedical applications. For instance, Hoffman and co-workers first applied PNIPAAm to drug delivery systems and the separation of substances from the surrounding aqueous medium [9, 10]. The function of PNIPAAm-conjugated enzymes was promoted or suppressed upon by temperature change due to sol–precipitate phase transition. Okano *et al.* extensively developed highly responsive synthetic polymer systems where reversible themoresponsiveness occurs rapidly upon a very abrupt temperature change. Previous studies on thermoresponsive polymer surfaces are as follows: (1) mixed PNIPAAm/Type I collagen solution coating (Takezawa *et al.* [2]), (2) PNIPAAm electron-beam-induced polymerization on surfaces (Okano *et al.* [3, 11, 12]) and (3) RGD-peptide-derivatized PNIPAAm solution coating (Matsuda and Moghaddam [6, 7]). Methods (I) and (III) are applicable to solution coating for devices of any shape, whereas method (II) is limited to electron-beam irradiated-portions but is favorable for miroprocessing.

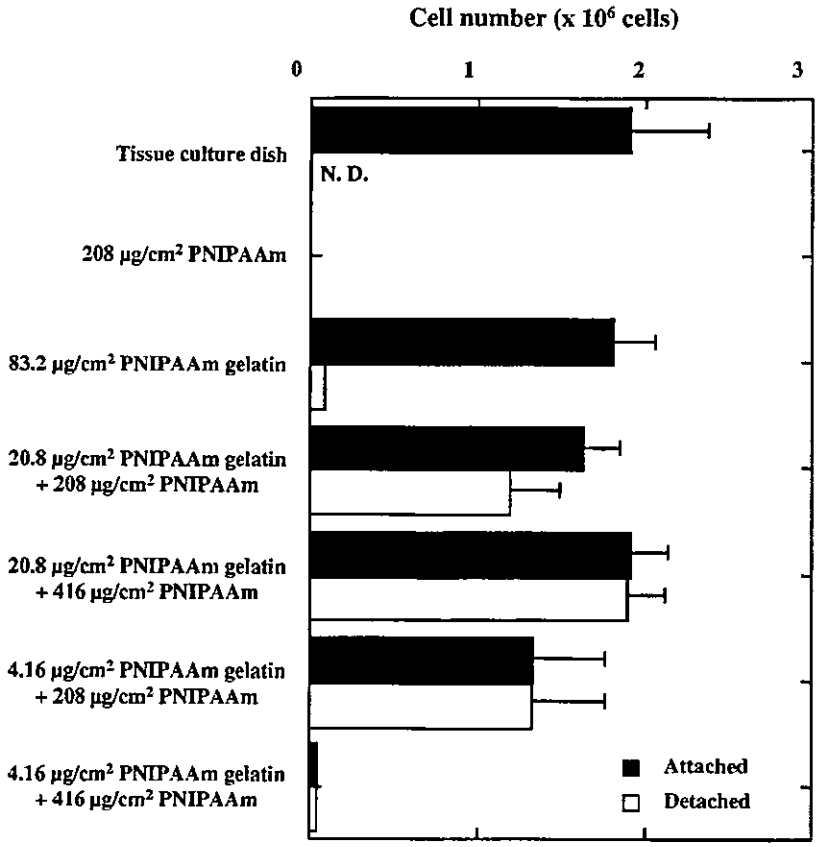

Figure 4. Attached cell number at 37°C and detached cell number at 20°C of ECs on surfaces coated with a mixture of PNIPAAm and PNIPAAm-grafted gelatin at different mixed ratios. N.D.; Not detectedable.

The new thermoresponsive cell adhesive matrix designed in this study was PNIPAAm-grafted gelatin. Gelatin, a thermally denatured collagen, has been utilized as a matrix protein similar to collagen and fibronectin. Graft polymerization was based on the photo-inferter polymerization technique, originally developed by Otsu *et al.* in the early 1980s. This unique photo-characteristic of the benzyl dithiocarbamate group leads to 'living-like' radical polymerization. Upon UV irradiation leading to photocleavage, a radical pair was generated but spontaneously recombined. The generated benzyl radical can initiate radical polymerization, whereas the counter radical, a dithiocarbamate radical, cannot attack vinyl monomers; rather, it tends to recombine with a growing polymer. Therefore, if side reactions such as chain transfer or recombination between polymer radical ends are markedly inhibited, a 'living-like' polymer will be produced. A series of studies by Otsu *et al.* [13, 14] and our previous studies [15, 16] have shown that polymer chain length increases with monomer concentration and irradiation time under appropriate conditions. In this study, the dithiocarbamate group was partially derivatized to react with the amine group of lysine residues of gelatin.

The molecular weight of PNIPAAm gel chain and the degree of substitution for PNIPAAm-gelatin (I) and (II) are listed as follows: for PNIPAAm-gelatin (I),

the average molecular weight of grafted gelatins is 1.4×10^4. The weight ratio of the grafted PNIPAAm chain to the gelatin molecule is approximately 0.5 and the average molecular weight of grafted chains is 1.5×10^3, assuming that all the derivatized photoinitiation participates in the graft polymerization. For PNIPAAm-gelatin (II) the molecular weight is approximately 3.8×10^5 g/mol, the weight ratio of the grafted chain to the gelatin molecule is approximately 3.0, and the average molecular weight of grafted chains is 1.1×10^4 g/mol. LCTSs of these grafted gelatins were slightly higher than that of PNIPAAm. However, in contrast to PNIPAAm, complete dissolution and precipitation, as determined from optical transmittance, was not obtained for these modified gelatins, suggesting that, although PNIPAAm chains collapsed at temperatures above LCST, gelatin molecules appeared to protect intramolecular aggregation, thus avoiding the complete precipitation in the diluted state at the concentration of 1.0 mg/ml in this study.

The thermoresponsiveness of cell adhesion is summarized as follows. Little cell adhesion occurs on PNIPAAm-coated or PNIPAAm/gelatin-mixture-coated dishes, whereas cell adhesion occurs on only PNIPAAm-gelatin (II)-coated surfaces, which results in the formation of a confluent monolayered sheet. However, complete delamination was not observed (Note that it has been reported that gelatin coating on dishes induces little desorption of gelatin as observed for commercial dishes). This might be due to the hydrophobic interaction between water-soluble PNIPAAm-gelatin and the non-treated polystyrene dish. In a separate experiment, gelatin coating (50 $\mu g/cm^2$) induced cell adhesion similarly to non-coated TCPS dishes. However, little delamination at room temperature within 20 min was observed. When a mixed ratio of PNIPAAm-gelatin and PNIPAAm was high, enhanced cell adhesion but reduced detachment was observed (Fig. 4). When the mixed ratio was very low, no adhesion was observed. Therefore, an optimal ratio appeared to exist for complete adhesion at 37°C and complete delamination at 20°C. As can be shown in Fig. 4, the mixed ratio of PNIPAAm-gelatin against PNIPAAm of 0.01 fulfilled the requirements mentioned above, indicating that a very small amount of PNIPAAm-gelatin in the mixture induced cell adhesion and spreading and full detachment at room temperature. Thus, the mixed ratio of cell-adhesive matrix (PNIPAAm-gelatin) and non-cell-adhesive matrix (PNIPAAm)greatly affects the balance of capabilities of cell adhesion at physiological temperature and cell detachment at room temperature.

Collagen and gelatin are key biological substances in biomaterials for cell adhesion, tissue formation and organ construction *in vitro* as well as *in vivo*. Collagen forms gels in physiological environments (pH and temperature) due to fiber formation and subsequent self-assembled fiber bundles, whereas gelatin at high concentration forms gels when temperature is lowered to room temperature due to enhanced intramolecular association resulting in the formation of an intramolecular random network with partial fiber formation, whereas at elevated temperature, dissolution occurs. This is a major drawback of the use of gelatin as a biomaterial

since gelatin is dissolved in water at physiological temperature. On the other hand, chemical crosslinking using glutaraldehyde is often used to render gelatin insoluble. In this paper, the designed synthetic polymer-conjugated gelatin has the so-called 'inversion temperature' phenomenon in which the polymer is dissolved at low temperature, but precipitated at physiological temperature. This is particularly important for cell embedding in tissue-engineered devices, as has been found for collagen. In addition, a solution-coatable, thermoresponsive cell matrix may have versatile applications. Such tissue-engineered applications will be reported in the near future.

Acknowledgement

The authors appreciate financial support by the Promotion of Fundamental Studies in Health Science of the Organization for Pharmaceutical Safety (OPSR) under Grant No. 97-15.

REFERENCES

1. M. Heskins and J. E. Guillet, *J. Macromol. Sci. Chem.* **A2**, 1441 (1968).
2. T. Takezawa, Y. Mori and K. Yoshizato, *Biotechnology* **8**, 854 (1990).
3. N. Yamada, T. Okano, H. Sakai, F. Karikusa, Y. Sawasaki and Y. Sakurais, *Makromol. Chem. Rapid. Commun.* **11**, 571 (1990).
4. T. Takezawa, M. Yamazaki, Y. Mori, T. Yonaha and K. Yoshizato, *J. Cell Sci.* **101**, 495 (1992).
5. T. Okano, N. Yamada, H. Sakai and Y. Sakurai, *J. Biomed. Mater. Res.* **27**, 1243 (1993).
6. T. Matsuda and M. J. Moghaddam, Molecular design of artificial fibrin glue, *Materials Science and Engineering* **C1**, 37–43 (1993).
7. M. J. Moghaddam and T. Matsuda, *ASAIO Trans.* **37**, 437–438 (1991).
8. R. Fields, *Biochem. J.* **124**, 581–590 (1971).
9. L. C. Dong and A. S. Hoffman, in: *ACS Symp. Ser. Vol. 350*, p. 236. American Chemical Society, Washington, DC (1987).
10. M. Miura, C.-A. Cole, N. Monji and A. S. Hoffman, *J. Biomater. Sci. Polymer Edn* **5**, 555–568 (1994).
11. H. Hirose, O. H. Kwon, M. Yamato, A. Kikuchi and T. Okano, *Biomacromolecules* **1**, 377 (2000).
12. A. Kushida, M. Yamato, C. Konno, A. Kikuchi, Y. Sakurai and T. Okano, *J. Biomed. Mater. Res.* **45**, 355 (1999).
13. T. Otsu and M. Yoshida, *Chem. Rapid. Commun.* **3**, 127 (1982).
14. T. Otsu and A. Matsumoto, *Adv. Polym. Sci.* **136**, 75 (1998).
15. Y. Nakayama and T. Matsuda, *Macromolecules* **32**, 5405 (1999).
16. H. J. Lee, Y. Nakayama and T. Matsuda, *Macromolecules* **32**, 6989 (1999).

Liquid photocurable biodegradable copolymers: *In vivo* degradation of photocured poly(ε-caprolactone-*co*-trimethylene carbonate)

Manabu Mizutani, Takehisa Matsuda
Department of Bioengineering, National Cardiovascular Center Research Institute, 5-7-1 Fujishiro-dai, Suita, Osaka 565-8565, Japan

Received 27 July 2001; revised 13 November 2001; accepted 5 December 2001

Abstract: Liquid photoreactive poly(ε-caprolactone-*co*-trimethylene carbonate)s endcapped with a coumarin group [coumarinated poly(CL/TMC)s] were prepared using tetrafunctional hydroxylated substances such as pentaerythritol or four-branched poly(ethylene glycol), b-PEG. These coumarinated copolymers are tetra-branched and exist as a viscous liquid (MW 5×10^3–7×10^3). They were photocured by ultraviolet (UV) light irradiation to obtain a swelling or non-swelling solid under water, depending on the type of initiator used. The resultant films were implanted into the subcutaneous tissues of rats for up to 5 months. The photocured b-PEG-based copolymer was completely degraded and sorbed within a 1 month. On the other hand, surface-eroding degradation of pentaerythritol-based, coumarinated poly(CL/TMC) progressed with implantation time, and minimal recruitment of neutrophils, macrophages, and multinucleated giant cells was observed over the implantation period. Among the pentaerythritol-based copolymers, the fastest surface erosion was observed for the copolymer with the highest ε-caprolactone content. Microfabricated films with microarrays in which photoconstructs were stereolithographically prepared, using three different coumarinated copolymers at different regions, showed that upon implantation there was regionally differentiated biodegradation of microarrays, and the degree of region-specific biodegradation depended on the type of photocured copolymer. The observed tendency for biodegradation was in good agreement with that observed during implantation of individual films *in vivo*. This study also demonstrates that the use of multi-material-arrayed films enables the determination of different responses *in vivo* using only one sample. © 2002 Wiley Periodicals, Inc. J Biomed Mater Res 61: 53–60, 2002

Key words: biodegradation; ε-caprolactone; trimethylene carbonate; photocured film; *in vivo* degradation

INTRODUCTION

Biodegradable poly(ester)s such as poly(lactide) or poly(glycolide) and their copolymers have been used as drug-delivery matrices, templates, and scaffolds in biomedical applications with a focus on the development of regenerative or reparative medicines.[1–4] These materials have been processed to make fibers, sheets, and blocks by solution-casting or melt-compression-mold techniques. If such biodegradable polymers are liquid and photocurable, a photochemically driven process can be utilized for manufacturing such forms of photocured materials as well as for direct three-dimensional (3D) fabrication of devices using a stereolithographic rapid prototyping method.[5–7]

Our recent efforts have been focused on designing photochemical liquid biomaterials and developing a photocuring fabrication process that would lead to the realization of a 3D photoconstruct with controlled surface erosion characteristics.[8–10] The designed liquid copolymers are four-armed copolymers composed of ε-caprolactone (CL) and trimethylene carbonate (TMC).[11–15] These four-armed copolymers are prepared by ring-opening addition reaction of cyclic compounds (CL and TMC) initiated with a four-functionality hydroxylated substance (pentaerythritol or four-branched PEG). Each terminal group of an arm was end-capped with a photodimerizable group, coumarin (Fig. 1).[8] The resultant photocurable copolymers

Correspondence to: T. Matsuda at Department of Biomedical Engineering, Graduate School of Medicine, Kyushu University, 3-1-1 Maidashi, Higashi-ku, Fukuoka 812-8582, Japan; e-mail: matsuda@med.kyushu-u.ac.jp

Contract grant sponsor: Promotion of Fundamental Studies in Health Science of the Organization for Pharmaceutical Safety and Research (OPSR); contract grant number: 97-15
Contract grant sponsor: Johnson & Johnson Medical Japan (Tokyo, Japan) (to MM)

were designated as coumarinated poly(CL/TMC). Ultraviolet (UV) irradiation induced inter- and intramolecular dimerization, resulting in chain extension and crosslinking.

In our previous article, we reported the synthesis and photocuring characteristics of these copolymers[8] and described in detail the *in vitro* hydrolytic behavior of photocured films.[10] In this paper, as an extension of a series of our study, we report the *in vivo* biodegradation characteristics of these photocured copolymers and the composition dependency of biodegradability.

MATERIALS AND METHODS

General procedure

All the solvents and reagents were purchased from Wako Pure Chemical Industries, Ltd. (Osaka, Japan) or Sigma-Aldrich Japan, Inc. (Tokyo). Diglycerol polyoxyethylene glycol ether (b-PEG) was obtained from Shearwater Polymers, Inc. (Alabama). Trimethylene carbonate (TMC) was prepared according to the method previously reported, and recrystallized from a mixture of ethyl acetate and hexane.[8,11] Also according to the method described in our previous paper,[8] 7-chlorocarbonyl methoxy coumarin was prepared for this study. Pentaerythritol was recrystallized from acetone. The other solvents and reagents were purified by distillation. ^{1}H NMR spectra were recorded on a JEOL JNM-GX270 FT-NMR spectrometer (270 MHz; Tokyo). The chemical shifts were given in δ values from Me_4Si as an internal standard. UV absorption spectra were measured on a JASCO Ubest-30 UV/VIS spectrometer (Tokyo). UV light (250-W Hg-Xe lamp; Hamamatsu Photonics L5662-02, Shizuoka, Japan) was irradiated through a Pyrex filter. The intensity of the UV light was measured at 250 nm on a TOPCON UVR-25 (Tokyo). The surface topographic changes of the photocured film were determined by scanning electron microscopy (SEM; JEOL JSM-6301F, Tokyo). Histologic observation was carried out by light microscopy (Olympus VANOX-S AHBS, Tokyo).

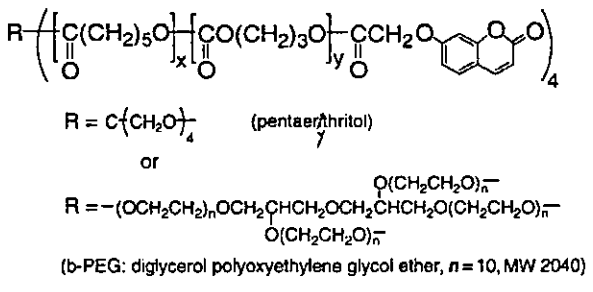

Figure 1. Photocurable, tetra-branched, biodegradable liquid copolymers.

Synthesis of coumarin-endcapped poly(ε-caprolactone-*co*-trimethylene carbonate) copolymer [coumarinated poly(CL/TMC)]

The preparation of coumarinated poly(CL/TMC) was carried out according to the method previously reported.[8–10] At first, poly(CL/TMC)s were prepared using trimethylpropane, pentaerythritol, or b-PEG as an initiator and tin(II)2-ethylhexanoate as a catalyst at almost full conversion (yield ~100%). Subsequently, hydroxyl groups at terminal ends of copolymers were esterified using 7-chlorocarbonyl methoxy coumarin. The composition of the copolymer was determined by ^{1}H-NMR spectroscopy, and the coumarin content of the coumarin-endcapped copolymer was determined by UV spectroscopy at an ε_{max} of 1.35×10^4.

Synthesis of coumarinated poly(2-hydroxyethyl methacrylate) (CPHEMA)

The preparation of CPHEMA was carried out by esterification of hydroxyl groups of HEMA (MW 3×10^5) using 7-chlorocarbonyl methoxy coumarin. Complete coumarination was qualitatively determined by IR spectroscopy (Shimadzu DR-8020, Kyoto). The photocured CPHEMA was used as a base polymer for the microarrayed architecture.

Preparation of photocured films

For individual photocured films, a liquid coumarinated poly(CL/TMC) (0.050 g, 0.3 mm in thickness) film (diameter, 11 mm) was prepared by casting dichloromethane solution on a cover glass, followed by air-drying. Subsequently, UV light irradiation was carried out for 60 min at an intensity of 10 mW/cm^2. (This condition enables complete conversion or curing, as reported in our previous paper[8].)

A micropatterned surface in which three different photocured copolymers were layered on the photocured CPHEMA film as a base substrate was prepared as schematically illustrated in Figure 2. A liquid coumarinated copolymer was coated on the photocured CPHEMA film and subsequently UV-irradiated using a moving light pen (light irradiation area: 1.0 mm in diameter) controlled by a custom-designed stereolithographic or rapid prototyping apparatus (SLA). A more detailed description of the device and photoirradiation conditions is given in our previous paper[8]. The height of the liquid film was 0.07 mm for one cycle, and the procedure was reported for up to three cycles, resulting in a bank (length, 5.0 mm; width, 1.0 mm; height, 0.2 mm) on the photocured CPHEMA surface. The sequential procedures using the second and the third liquid copolymers at different surface regions resulted in the formation of three different microbanks on the photocured CPHEMA surface.

Water adsorptivity and surface wettability

The photocured film, prepared as above, was immersed in water for 2 days at room temperature. The degree of water

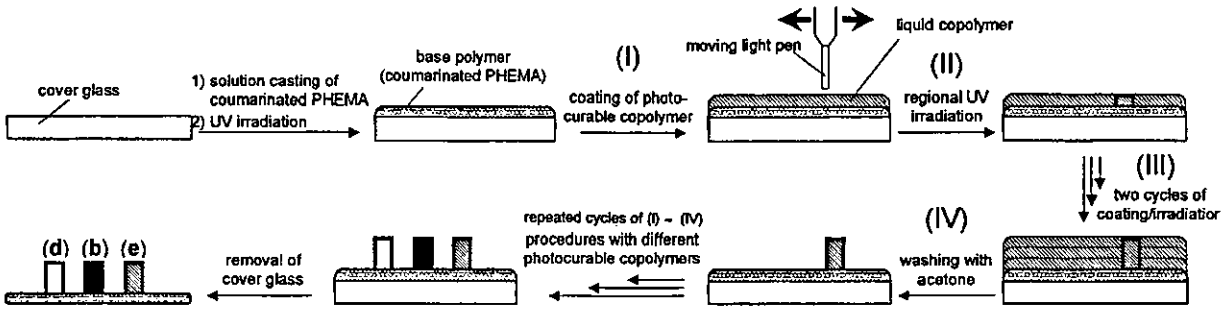

Figure 2. Preparation of a multiarrayed film by sequential steps using a custom-designed stereolithographic apparatus.

adsorptivity (DW) was determined as the relative amount of water uptake, on a weight basis, as measured against a dry photocured copolymer. The surface wettability of the films was determined by advancing and receding contact angles measured with a contact angle meter (Kyowa Interface Co. Ltd., Tokyo) at 25°C by the sessile drop method.

In vivo implantation

Round-shaped photocured films (diameter, 11 mm) that had been washed with ethanol and air-dried were implanted under the dorsal skin of male Wistar rats (around 400 g in weight). After a predetermined time, the rats were dissected to remove the films together with surrounding tissues. The films, which were easily removed from surrounding tissues, were thoroughly washed with water, freeze-dried, and weighed. The surrounding tissues were fixed in 1% aqueous formaldehyde aqueous solution (pH 7.4) for 12 h and stained with hematoxylin–eosin (HE) and periodic acid Schiff (PAS). The schematics of the stereolithographic photoconstruct procedures are shown in Figure 2.

RESULTS

Figure 1 shows the molecular structure of coumarinated poly(CL/TMC)s. Table I summarizes the molecular descriptions of the liquid copolymers used in this study. The copolymers of CL and TMC were prepared by ring-opening polyaddition reaction using a tetra-functional hydroxylated substance—pentaerythritol or diglycerol polyoxyethylene glycol ether (b-PEG)—as an initiator. The reaction was performed to achieve approximately 100% yield. Therefore the copolymer compositions were identical to those of the initial feed compositions.

Subsequent endcapping with 7-chlorocarbonyl methoxy coumarin was carried out according to the method described in our previous papers[8–10] in which reaction conditions and characterization of copolymers were described in detail. The content of CL in the copolymers ranged from 0 to 0.76 (molar ratio). All the coumarinated poly(CL/TMC)s were viscous liquid, and the average molecular weights of these copolymers ranged from 5×10^3 to 7×10^3. The degree of water adsorption of completely photocured films at the equilibrium state was approximately several percent of the dry weight for pentaerythritol-initiated copolymers, irrespective of copolymer composition (**a–d**, Table I). On the other hand, the b-PEG-initiated copolymer adsorbed water at about 60 percent of the dry weight (**e**, Table I). (Note that complete curing under reaction conditions was confirmed in a separate experiment.[8])

The round-shaped, photocured films (diameter, 11 mm; thickness, 0.3 mm) were implanted under the dorsal skin of rats. Table II shows the implantation-period-dependent loss of weight of the photocured films. The PEG-based photocured copolymer film was

TABLE I
Molecular Descriptions of Coumarin-Endcapped Tetra-Branched Biodegradable Liquid Copolymers, Coumarinated poly(CL/TMC)

Polymer Code Name	Initiator[a]	Copolymer Composition CL : TMC[b]	Coumarin Content (mol/g)	M_w^c	DW[d]
a	$C(CH_2OH)_4$	0.76 : 0.24	8.07×10^{-4}	5.0×10^3	0.03
b	$C(CH_2OH)_4$	0.49 : 0.51	7.90×10^{-4}	5.1×10^3	0.03
c	$C(CH_2OH)_4$	0.27 : 0.73	8.04×10^{-4}	5.0×10^3	0.05
d	$C(CH_2OH)_4$	0.00 : 1.00	8.00×10^{-4}	5.0×10^3	0.07
e	b-PEG[e]	0.49 : 0.51	5.71×10^{-4}	7.0×10^3	0.58

[a]Molar fraction of monomer per total OH group of initiator was fixed at 6.6; [b]composition ratio of CL and TMC (molar ratio); [c]molecular weight was estimated from coumarin content; [d]degree of water adsorptivity (relative weight of water uptake to polymer) of photocured film; [e]tetra-branched-PEG (diglycerol polyoxyethylene glycol ether) (MW 2040).

TABLE II
Weight Loss of Implanted Photocured Films as a Function of Implantation Period[a]

Polymer Code Name	Coumarinated Copolymer		1 Month		3 Months		5 Months	
			Weight Loss		Weight Loss		Weight Loss	
	Initiator	CL: TMC[b]	(%)	(mg/cm^2)	(%)	(mg/cm^2)	(%)	(mg/cm^2)
a	$C(CH_2OH)_4$	0.76 : 0.24	—	—	44.9 (8.4*)	8.2 (0.8*)	—	—
b	$C(CH_2OH)_4$	0.49 : 0.51	2.5 (2.8*)	0.4 (0.2*)	8.8 (6.9*)	1.7 (0.5*)	37.8	7.2
c	$C(CH_2OH)_4$	0.27 : 0.73	—	—	9.4 (7.0*)	1.7 (0.5*)	—	—
d	$C(CH_2OH)_4$	0.00 : 1.00	3.2 (2.2*)	0.6 (0.2*)	10.7 (3.6*)	1.7 (0.3*)	56.5	9.8
e	b-PEG[c]	0.49 : 0.51	100 (12.0*)	>12 (0.9*)	—	—	—	—

[a]Round photocured films: diameter 11 mm, thickness 0.3 mm; [b]compositional ratio of CL and TMC (molar ratio); [c]tetra-branched-PEG (diglycerol polyoxyethylene glycol ether) (MW 2040); *numbers in parentheses are weight losses determined in *in vitro* observation in pH 7.4 phosphate buffer aqueous solution (reported previously[10]).

completely lost at 1 month after implantation due to complete degradation and sorption. However, the pentaerythritol-based copolymer films maintained their integrity without shape change even at 3 months after implantation.

The biodegradation behavior of two photocured copolymers (**b** and **d**) was determined through time-lapse examination. Both copolymers progressively degraded with time, irrespective of composition. That is, at the early period of implantation (1 month), weight loss (per volume as well as per unit area) was very small, but considerable weight loss was observed at 5 months after implantation. At 3 months after implantation, the copolymer with the highest CL content (**a**: CL content of 76%) was degraded to a much greater degree than the others. There was little significant difference in the degree of degradation among the three remaining copolymers (CL content: 0~49%, **b**, **c**, and **d**). At 5 months after implantation, approximately 40–60% weight loss was observed for the copolymers **b** and **d**.

Upon implantation, surfaces became very slippery, probably due to surface erosion, and the implanted surfaces with surrounding tissues could not be harvested from the tissues. However, the implanted films were easily detached from the living tissue and were thoroughly washed with water. These surfaces became highly wettable with water. At 1 month after implantation, the receding contact angle was as low as several degrees (Table III).

Scanning electron microscopy observation showed that the surfaces, which were very smooth before implantation, had become rough after 1 month of implantation (Fig. 3). At 3 months after implantation, the surfaces were visibly roughened, and at 5 months after implantation they were significantly eroded, forming wide roughened surfaces.

Figure 4 shows histologic sections of the implanted copolymer **b** films at 1, 3, and 5 month(s) after implantation. At 1 month [Fig. 4(A)], little inflammatory reaction without recruitment of neutrophils and encapsulation of surrounding tissues was noted. At 3 months (Fig. 4(B)], a few giant cells had appeared. At 5 months [Fig. 4(C)], giant cells had accumulated at the interface where cells tended to invade into the photocured copolymer that was being degraded.

Histologic sections of tissues implanted with three different copolymers (**a**, **c**, and **d**) for 3 months are shown in Figure 5. With regard to the copolymer with the highest CL content (**a**), a massive foreign-body-induced tissue reaction has occurred: multinucleated giant cells have accumulated at the implant surface, which has become rough due to degradation. The roughened tissue surface oriented towards the film indicates a cellular ingrowth to surface regions rich with neutrophils [purple colored upon staining by PAS; Fig. 5(B)]. There was little appreciable difference in the tissue reactions between copolymers **b** and **c**, as shown in Figure 4(C,D).

At 5 months after implantation, accelerated degradation of the films was observed to promote tissue reaction, with giant cells migrating into biodegrading films. The integrity of the implanted film was lost, irrespective of the type of film (data not shown).

TABLE III
Surface Wettability of Photocured Films

Polymer Code Name	Coumarinated Copolymer		Water Contact Angle[b] (Degree) Advancing/Receding	
	Initiator	CL: TMC[a]	Before Implantation	1 Month After Implantation
b	$C(CH_2OH)_4$	0.49 : 0.51	65/44	52/<5
d	$C(CH_2OH)_4$	0.00 : 1.00	52/24	22/<5

[a]Compositional ratio of CL and TMC (molar ratio); [b]experimental error was ± 5%.

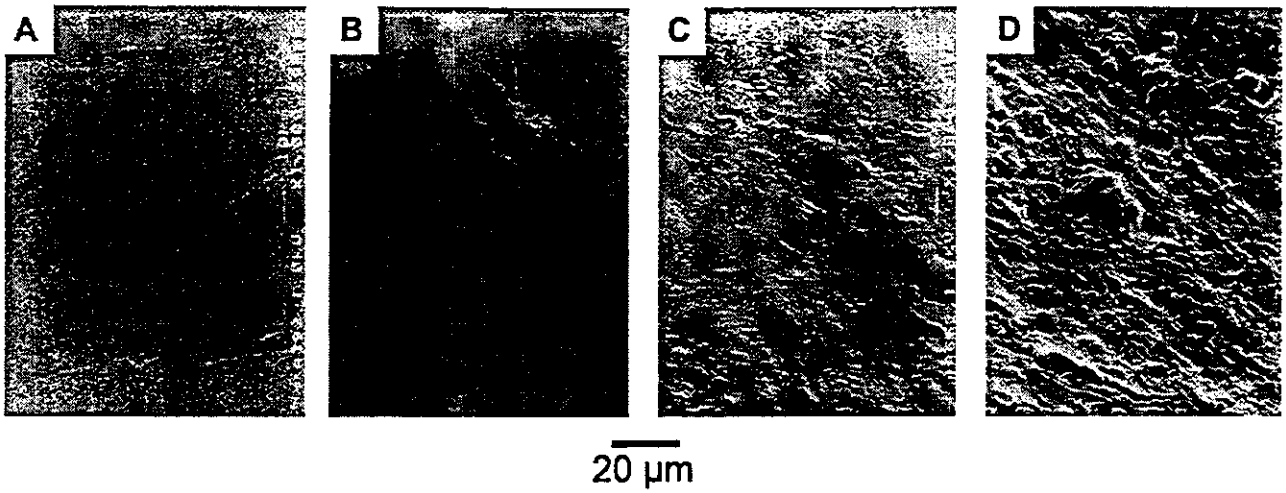

Figure 3. SEM images of the surfaces of photocured copolymer **b** (polymer code in Table I) film before and after implantation for up to 5 months: (A) before implantation, (B) after 1 month of implantation, (C) after 3 months of implantation, and (D) after 5 months of implantation.

Stereolithographically prepared microarchitectured films, on which three different photocured copolymer (**b**, **d**, or **e**)-based microarrays were constructed, were implanted into the subcutaneous tissues of rats. Figure 2 illustrates the sequential procedures for microfabrication. First, coumarinated poly(HEMA), CPHEMA, was coated and photocured on the glass as a base photocured construct on which a viscous photocurable copolymer was overlaid. A motor-driven light pen, controlled by computer-assisted software, was scanned and photoirradiated on the liquid-filled surface. After one array was prepared, the first liquid photocurable copolymer was wiped off the surface, and then the second liquid photocurable copolymer was overlaid, and photocuring was repeated at different regions. Repetition of the cycle three times produced a total of three microarrays (height, 0.2 mm; length, 5. 0 mm; width, 1. 0 mm) with three different copolymers (**b**, **d**, and **e**, Table I). Upon subcutaneous implantation of the prepared microarray films, different responses in term of biodegradability were observed for each microarray by scanning electron microscopy (Fig. 6).

At 1 month after implantation, complete loss of the PEG-based copolymer **e** was observed. Some surface erosion appeared to occur for copolymers **b** and **d** [Fig. 6(B)]. Irrespective of the type of copolymer (**b** or **d**), at 3 months after implantation, surface erosion pro-

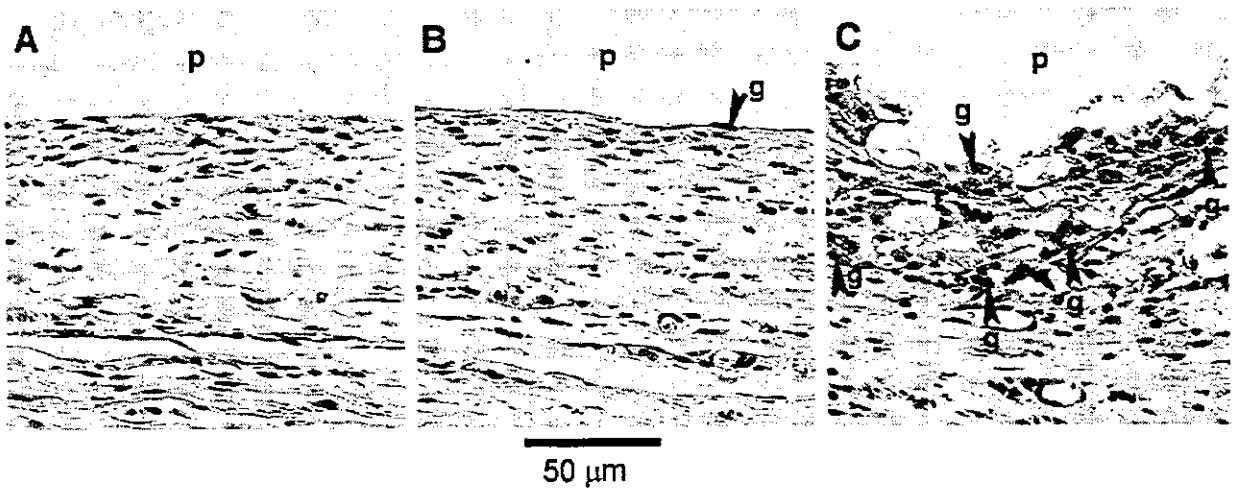

Figure 4. Histologic cross-sectional photographs of photocured copolymer **b** (polymer code in Table I) film facing subcutaneous tissues after 1 week of implantation: (A) after 1 month of implantation, (B) after 3 months of implantation, and (C) after 5 months of implantation. All the specimens were stained by H&E. p = the space occupied by the photocured film (note that the photoconstruct film became very slippery due to surface hydrolysis and spontaneously detached at the time of retrieval); g = multinucleated, giant cells.

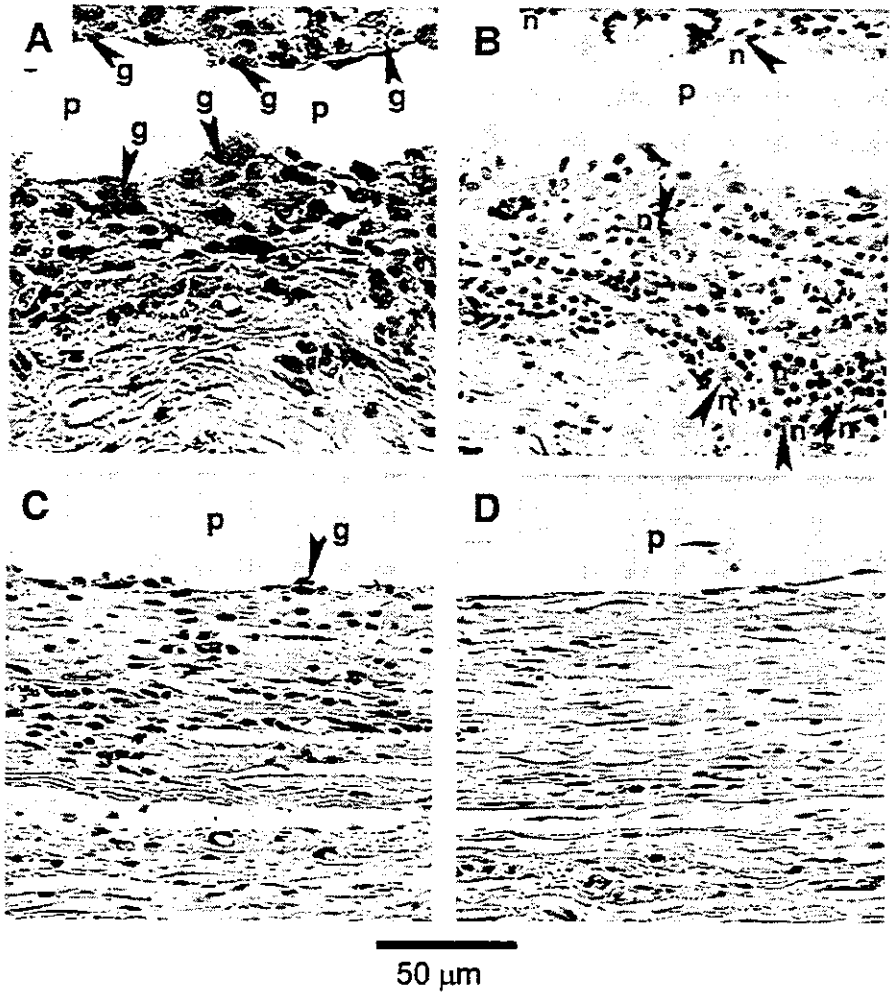

Figure 5. Histologic cross-sectional photographs of photocured film facing subcutaneous tissues after 3 months of implantation (p = the space occupied by the photocured film). As shown, the implanted copolymer films are: (A) and (B) (copolymer **a** in Table I), (C) (**c** in Table I), and (D) (**d** in Table I). The specimens were stained by H&E, except for (B), which was PAS stained. g = multinucleated, giant cells; n = purple neutrophils upon PAS staining.

ceeded without any partial destruction or loss of the integrity of the entire photoconstruct [Fig. 6(C)]. At 5 months after implantation, the thickness of the photoconstructs was significantly reduced and only traces of the photoconstructs remained on the surface [Fig. 6(D)].

DISCUSSION

The nature of surface erosion of implant devices, if it occurs synchronously with tissue ingrowth or regeneration, may be beneficial for replacement of diseased or lost tissues with artificial devices or with cell-incorporated, tissue-engineered devices. In such cases, the mechanical and structural integrity of implanted scaffolds and templates could be well maintained during the tissue architecture. That is, the degenerating integrity of surface-eroded scaffolds with implantation time would be complemented by the regenerating integrity of ingrown tissue. We have devised a photocuring system and developed a photofabrication process using a liquid biodegradable copolymer composed of CL and TMC. In a copolymer, both monomer units are susceptible to hydrolysis, and coumarination at the terminal ends of liquid poly(CL/TMC)s produces an insoluble photocured solid upon photoirradiation.[8]

A survey of patents indicated that liquid biodegradable copolymers are useful as filling materials for soft-tissue defects.[11–14] The literature has reported that poly(TMC) is much less susceptible to hydrolysis than poly(CL) in both *in vitro* and *in vivo* conditions.[15] Our previous study showed that the hydrolysis rate in slightly alkaline aqueous solution (pH 8.7) decreased with an increase in the TMC content of copolymers.[10] On the other hand, the *in vivo* enzymatic surface ero-

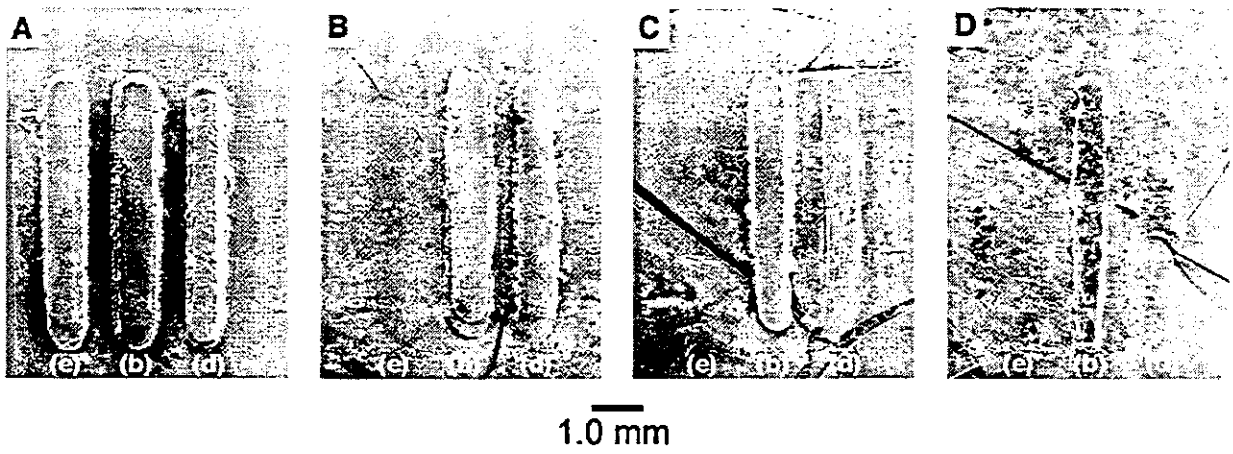

Figure 6. SEM images of multiarrayed film before and after implantation for up to 5 months: (A) before implantation, (B) after 1 month of implantation, (C) after 3 months of implantation, and (D) after 5 months of implantation. **e**, **b**, and **d** correspond to polymer code names in Table I.

sion of synthetic polymers is a relatively rare process, with only a few examples reported in the literature, such as poly(TMC). The contribution of an enzymatic process to the degradation of poly(TMC) *in vivo* was supported by a much higher rate of chain scission and mass loss, relative to *in vitro* degradation.[15]

The present *in vivo* degradation study of subcutaneous implantation of photocured films in rats shows that among photocured films, including photocured coumarinated poly(CL/TMC)s with compositional CL/TMC ratios of 75/25, 50/50, and 25/75 and poly(TMC), the highest degradability at an early implantation time (~3 months) was observed for the copolymer with the highest CL content (copolymer a).

Except for copolymer **a**, there appeared to be little significant difference in degradability among the copolymers in terms of gravimetric mass change and tissue reactions. At 5 months after implantation, surface erosion proceeded irrespective of the copolymers, resulting in considerable mass loss and integrity, and cell phagocytes, such as macrophages, appeared on the substrate oriented towards the tissue layers. Occasionally, multinucleated giant cells were observed. Fibrosis appeared to be minimal, suggesting that surface erosion proceeded without significant adverse tissue reactions.

In vitro alkaline hydrolysis experiments showed that there is a marked dependency of copolymer compositions on the hydrolysis rate,[10] but the *in vivo* study showed that, except for high-CL-content copolymers **c** and **d**, there appears to be no significant difference. This may be due to the synergistic effect of hydrolysis and enzymatic degradation. This is in good accordance with the results obtained using a stereolithographically prepared microphotoconstruct on one surface, which was implanted in a subcutaneous tissue.

The advantage of using a microarrayed surface, the microarray of which is photoconstructed with different photocured copolymers, is that it enables the differentiation of biodegradation rates on one film. PEG-based poly(CL/TMC) (**e**) was found to be very biodegradable, the biodegradation appearing to proceed via both surface erosion and bulk degradation. This agrees well with the property of lactide-based PEG scaffolds.[4]

CONCLUSIONS

Liquid biodegradable copolymers composed of CL and TMC endcapped with a coumarin group may be useful for tailored-made and precision-shaped scaffolds or templates.

The authors thank Dr. Hatsue Ueda, Department of Pathology, National Cardiovascular Center Hospital, for her guidance, advice, and discussion on the histology section of this study. One of the authors (MM) appreciates the financial support from Johnson & Johnson Medical Japan (Tokyo, Japan) and the continuous encouragement of Dr. G. N. Kumar, Dr. S. C. Arnold, and Dr. A. G. Scopelianos, all of whom are from Johnson & Johnson.

References

1. Piskin E. Biodegradable polymers as biomaterials. J Biomater Sci, Polym Edn 1994;6:775–781.
2. Albertsson A.-C, Karlsson S. Degradable polymers for the future. Acta Polym 1995;46:114–119.
3. Whang K, Thomas CH, Healy KE. A novel method to fabricate bioabsorbable scaffolds. Polymer 1995;36:837–842.
4. Han DK, Park KD, Hubbell JA, Kim YH. Surface characteristics and biocompatibility of lactide-based poly(ethylene glycol) scaffolds for tissue engineering, J Biomater Sci, Polym Edn 1998;9:667–673.
5. Palser R, Jamieson R, Sutherland JB, Skibo L. Three-

dimensional lithographic model building from volume data sets. Can Assoc Radiol J 1990;41:339–345.
6. Kucybala Z, Pietzak M, Paczkowski J, Lindén LÅ, Rabek JF. Kinetic studies of a new photoinitiator hybrid system based on camphorquinone-N-phenylgline derivatives for laser polymerization of dental restorative and stereolithographic (3D) formulations. Polymer 1996;37:4585–4595.
7. Poulsen M, Lindsay C, Sullivan T, D'Urso P. Stereolithographic modelling as an aid to orbital brachytherapy. Int J Rad Oncol Biol Phys 1999;44:731–742.
8. Matsuda T, Mizutani M, Arnold SC. Molecular design of photocurable liquid biodegradable copolymers. I. Synthesis and photocuring characteristics. Macromolecules 2000;33:795–804.
9. Matsuda T, Mizutani M. Molecular design of photocurable liquid biodegradable copolymers. II. Synthesis of coumarin-derivatized oligo(methacrylate)s and photocuring. Macromolecules 2000;33:791–794.
10. Mizutani M, Matsuda T. Photocurable liquid biodegradable copolymers: *In vitro* hydrolytic degradation behaviors of photocured films of coumarin-endcapped poly([g<]ca-caprolactone-co-trimethylene carbonate). Biomacromolecules. Forthcoming.
11. Albertsson A.-C, Eklund M. Synthesis of copolymers of 1.3-dioxane-2-one and oxepan-2-one using coordination catalysts. J Polym Sci Part A, Polym Chem 1994;32:265–268.
12. Scopelianos AG, Bezwada RS, Arnold SC, Gooding RD. Liquid polymer filled envelopes for use as surgical implants. US Patent no. 5,411,554; July, 1993.
13. Scopelianos AG, Arnold SC, Bezwada RS, Roller MB, Huxel ST. Injectable microdispersions for soft tissue repair and augmentation. US Patent no. 5,599,852; October, 1994.
14. Bezwada RS, Arnold SC, Shalaby WS. Liquid absorbable copolymers for parenteral application. US Patent no. 5,653,992; April, 1995.
15. Zhu KJ, Hendren RW, Jensen K, Pitt CG. Synthesis, properties, and biodegradation of poly(1, 3-trimethylene carbonate). Macromolecules 1991; 24:1736–1742.

Thermoresponsive Heparin Coating: Heparin Conjugated with Poly(*N*-isopropylacrylamide) at One Terminus

Tomoko Magoshi,† Houcin Ziani-Cherif,† Shoji Ohya,† Yasuhide Nakayama,† and Takehisa Matsuda*,‡

Department of Bioengineering, National Cardiovascular Center Research Institute, 5-7-1, Fujishiro-dai, Suita, Osaka 565-8565, Japan, and Department of Biomedical Engineering, Graduate School of Medicine, Kyushu University, 3-1-1, Maidashi, Higashi-ku, Fukuoka 812-8582, Japan

Received September 7, 2001. In Final Form: February 4, 2002

Heparin terminally grafted with a thermoresponsive polymer, poly(*N*-isopropylacrylamide) (PNIPAM), was prepared by sequential steps of chemical modification of one terminal group of heparin, leading to its dithiocarbamylation as an iniferter (*ini*tiator−trans*fer* agent−*ter*minator), followed by quasi-living photopolymerization, thereby producing PNIPAM with a molecular weight (mol wt) ranging from 2×10^3 to 1×10^5 g/mol at the terminus of heparin (PNIPAM−heparin). The lower critical solution temperature depended on the mol wt of PNIPAM. Higher-mol-wt PNIPAM−heparin completely precipitated at 34 °C. The adsorptivity on the poly(ethylene terephthalate) (PET), poly(styrene) (PST), and segmented polyurethane (PU) films was assessed by wettability measurement and surface chemical compositional analysis using X-ray photoelectron spectroscopy. The temperature-dependent amount of adsorbed PNIPAM−heparin was quantitatively determined by a confocal laser scanning microscope (CLSM) using fluorescence-labeled PNIPAM−heparin. The relative degree of heparin complexation with antithrombin III (ATIII) was assessed based on fluorescence intensity using the avidin−biotinylated enzyme complex assay technique under a CSLM. The results showed that irrespective of the type of polymer films, higher-mol-wt PNIPAM−heparin adsorbed better and was more stable than lower-mol-wt PNIPAM−heparin at 40 and 20 °C, an effect which was more enhanced on a hydrophobic surface (PST) than on polar surfaces (PET and PU). The desorption of PNIPAM−heparin did not occur even in the serum-containing medium. In addition, higher complexation capability with ATIII was observed for higher-mol-wt PNIPAM−heparin probably due to its higher adsorption capability. The desorption of PNIPAM−heparin was noted at 20 °C. Thus, it is concluded that PNIPAM−heparin exhibits thermoresponsiveness of surface biofunctionality.

Introduction

Heparin, which is a glycosaminoglycan, has potent anticoagulant activity when complexed with antithrombin III (ATIII) and has been clinically used as an anticoagulant during extracorporeal circulation. Various heparinization techniques applicable to blood-contacting surfaces of extracorporeal devices or catheters have been proposed and developed. These include surface physical mixing,[1,2] coating with the surfactant−heparin complex,[3] surface derivatization through covalent bonding with or without a spacer arm,[4−7] impregnation into a surface hydrogel layer,[11] and complexation onto an animated surface.[8−10]

Physical adsorption is achieved by electrostatically or hydrophobically driven adsorption. In particular, we synthesized a novel "heparin surfactant", in which heparin is terminally derivatized with a long alkyl chain such as lauryl and stearyl groups.[12] Such a heparin surfactant is adsorbed on a polymer surface from an aqueous solution via a hydrophobically driven adsorption process. Physicochemical analyses suggested that the hydrophobic tail of alkylated heparin can anchor on a hydrophobic polymer surface and the heparin molecule is oriented vertically to aqueous media from the surface.

In this study, poly(*N*-isopropylacrylamide) (PNIPAM) with a lower critical solution temperature (LCST) of 32 °C[13] was grafted by polymerization of NIPAM from the dithiocarbamate group, an iniferter (photocleavable radical generator)[14] derivatized on the terminus of heparin. The bioconjugation of heparin and PNIPAM without substantial loss of their bioactivity may be used for adsorption-driven surface modification by simple coating using its aqueous solution at room temperature and concomitant physical stabilization on a substrate surface at a physiological temperature. In this study, we prepared such a thermoresponsive heparin conjugate (PNIPAM−

* To whom correspondence should be addressed. Tel: 81-92-642-6210. Fax: 81-92-642-6212. E-mail: matsuda@med.kyushu-u.ac.jp.

† National Cardiovascular Center Research Institute.

‡ Kyushu University.

(1) Kim, S. W.; Ebert, C. D.; Lin, J. Y.; McRea, J. C. *ASAIO J.* **1983**, *6*, 76−87.

(2) Goosen, M. F. A.; Sefton, M. V. *J. Biomed. Mater. Res.* **1979**, *13*, 347−364.

(3) Leninger, R. I.; Cooper, C. W.; Falb, R. D.; Grode, G. A. *Science* **1966**, *152*, 1625−1626.

(4) Ebert, C. D.; Kim, S. W. *Thromb. Res.* **1982**, *26*, 43−57.

(5) Yuan, S.; Cai, W.; Szakalas-Gratz, G.; Kottke-Marchant, K.; Tweden, K.; Marchant, R. E. *J. Appl. Biomater.* **1995**, *6*, 259−266.

(6) Larm, O.; Larsson, R.; Olsson, P. A. *Biomater., Med. Devices, Artif. Organs* **1983**, *11* (2−3), 161−173.

(7) Olsson, P.; Sanchez, J.; Mollnes, T. E.; Riesenfeld, J. *J. Biomater. Sci., Polym. Ed.* **2000**, *11*, 1261−1273.

(8) Holland, F. F.; Gidden, H. E.; Mason, R. G.; Klein, E. *Artif. Organs* **1978**, *1*, 24−36.

(9) Barbucci, R.; Baszkin, A.; Benvenuti, M.; de Lourdes Costa, M.; Ferruti, P. *J. Biomed. Mater. Res.* **1987**, *21*, 443−457.

(10) Tanzawa, H.; Mori, Y.; Harumiya, N.; Miyama, H.; Hori, M.; Oshimu, N.; Idezuki, Y. *Trans.−Am. Soc. Artif. Intern. Organs* **1973**, *19*, 188−194.

(11) Goosen, M. F. A.; Sefton, M. V. *J. Biomed. Mater. Res.* **1983**, *17*, 359−373.

(12) Matsuda, T.; Magoshi, T. *Biomacromolecules* **2001**, *2*, 1169−1177.

(13) Heskins, M.; Guillet, J. E. *J. Macromol. Sci., Chem.* **1968**, *A2*, 1441−1455.

(14) Otsu, T.; Matsumoto, A. *Adv. Polym. Sci.* **1998**, *136*, 75.

10.1021/la011408s CCC: $22.00
Published on Web 05/17/2002

heparin). Its complexation with ATIII was assessed with a confocal laser scanning microscope using an antibody–enzyme-based chromogenic substrate. In this paper, the preparation of PNIPAM-grafted heparin was described, followed by graft chain length dependency of its surface adsorption/desorption and biological activity characteristics.

Experiments

Reagents. 4-(Chloromethyl)benzoic acid and NIPAM were purchased from Tokyo Kasei Co. (Tokyo, Japan). ATIII and bovine serum albumin (BSA) were obtained from Sigma Chemicals Co. (St. Louis, MO). Other reagents and solvents were obtained from Wako Pure Chemicals Inc. (Osaka, Japan). The poly(ethylene terephthalate) (PET), poly(styrene) (PST), and segmented polyurethane (PU) films were obtained from Bellco Glass Inc. (Vineland, NJ), Minamide Corp. (Osaka, Japan), and Nihon Zeon Co. (Tokyo, Japan), respectively. All solvents and reagents were of special grade and used without further purification, except for NIPAM which was recrystallized from toluene–hexane and stored in the refrigerator.

General Methods. Purification of heparin, oxidized heparin, and PNIPAM–heparin was carried out using a dialysis membrane (molecular weight (mol wt) cutoff level = 12 000–14 000, Wako). The ion-exchange was performed using a Dowex 50 × 8 (H^+) resin (Dow Chemicals, Midland, MI). ^{1}H NMR spectra were recorded in $CDCl_3$ using tetramethylsilane as the internal standard with a JNM-GX270 FT-NMR spectrometer (JEOL, 270 MHz, Tokyo, Japan). UV/vis spectra were recorded using a Ubest-30 UV/vis spectrophotometer (Japan Spectroscopic Co., Ltd., Tokyo, Japan). X-ray photoelectron spectroscopy (XPS) was performed to determine the surface chemical composition using an ESCA-3400 instrument (Shimadzu Corp., Kyoto, Japan) at the takeoff angle of 90°. Wettability of the treated surfaces was evaluated using the sessile drop technique with a contact angle meter (CA-D, Kyowa Interface Science Co., Ltd., Saitama, Japan). The fluorescence image of the surface was observed using a confocal laser scanning microscope (MRC-1024, 543 nm exDitation; Bio-Rad Lab., Hercules, CA).

Synthesis of Lactone-Terminated Heparin [2]. The detailed preparation is according to the method described by Sugiura et al.[15] Heparin sodium salt (4.0 g, mol wt = 1.2×10^4; 198.6 IU/mg) was dissolved in deionized water and passed through a Dowex 50 × 8 (H^+) column. The eluate was dialyzed and then lyophilized to yield heparin (3.8 g, 0.32 mmol). The reducing end of heparin was oxidized with iodide (0.8 g, mmol) in 20% aqueous methanol solution (100 mL) for 6 h at room temperature. The reaction solution was added to ethanol containing 4% potassium hydroxide (200 mL). The white precipitate was obtained by filtration and dissolved in deionized water, and the resulting solution was dialyzed. Upon freeze-drying of the dialyzed solution, oxidized heparin was obtained. The oxidized heparin was dissolved in deionized water and passed through a Dowex 50 × 8 (H^+) column. Upon freeze-drying of the eluate, lactone-terminated heparin [2] was obtained (3.0 g; yield, 78%).

4-(*N,N*-Diethyldithiocarbamoylmethyl)benzoic Acid [4]. Sodium *N,N*-diethyldithiocarbamate trihydrate (10.6 g, 46.9 mmol) and sodium iodide (4.4 mg, 2.9 mmol) were added to an ethanolic solution (150 mL) of 4-(chloromethyl)benzoic acid [3] (5.0 g, 29.3 mmol). The mixture was refluxed for 4 h and then stirred overnight at room temperature. After evaporation of ethanol, the crude mixture was neutralized with 10% cold aqueous hydrochloric acid solution and the product was extracted with ethyl acetate three times. The organic layer was dried using sodium sulfate, filtered with a pad of Celite, and evaporated under reduced pressure. The product of purification was confirmed by thin-layer chromatography (TLC). The results were as follows. Yield: 8.3 g, 99%. TLC: $R_f = 0.7$ ($CHCl_3/CH_3OH = 80/20$). ^{1}H NMR ($CDCl_3$, δ ppm): 8.04 (*d*, 2H, Ar-*H*), 7.48 (*d*, 2H, Ar-*H*), 4.63 (s, 2H, Ar–CH_2), 4.05 (*m*, 2H, CH_2N), 3.75 (*m*, 2H, CH_2N), and 1.29 (*t*, 6H, CH_3).

4-[(*N,N*-Diethyldithiocarbamoylmethyl)-2-aminoethyl]-benzamide [6]. Oxalyl chloride (5.0 mL, 58.2 mmol) and two drops of *N,N*-dimethylformamide (DMF) were added to a solution of acid **4** (6.6 g, 23.3 mmol). The mixture was stirred at room temperature for 3 h and then concentrated under reduced pressure. Addition of toluene (50 mL) followed by evaporation of the solution under reduced pressure was repeated twice to remove excess oxalyl chloride. Crude acid chloride [5] was then dissolved in methylene chloride (200 mL) and cooled to 0 °C in an ice bath. A solution of ethylenediamine (16 mL, 233 mmol) in methylene chloride solution (50 mL) was added dropwise with vigorous stirring at 0 °C, and the reaction mixture was stirred overnight at room temperature. The solvent was evaporated under reduced pressure, and the product was purified by silica gel column chromatography (elution: $CHCl_3/CH_3OH$ = 90/10 with $(CH_3CH_2)_3N$ (1%)). The results were as follows. Yield: 6.7 g, 88%. TLC: $R_f = 0.15$ ($CHCl_3/CH_3OH = 80/20$). ^{1}H NMR ($CDCl_3$, δ ppm): 7.74 (*d*, 2H, Ar-*H*), 7.43 (*d*, 2H, Ar-*H*), 6.83 (*s*, 1H, N*H*), 4.59 (*s*, 2H, CH_2S), 4.04 (*m*, 2H, CH_2N), 3.70 (*m*, 2H, CH_2N), 3.49 (*m*, 2H, CH_2N), 2.94 (*m*, 2H, CH_2N), 1.99 (*s*, 2H, NH_2), and 1.28 (*t*, 6H, CH_3).

Heparin Derivatized with Dithiocarbamate Iniferter [7]. Compound **6** (162 mg, 5.0×10^{-4} mol) in DMF (5.0 mL) was added to lactone-terminated heparin (300 mg, 0.025 mmol) solution in DMF (17 mL) and then neutralized with tri-*n*-butylamine (0.1 mL). The mixture was stirred for 16 h at 80 °C under an argon atmosphere. After evaporation of the solvent under vacuum, the residue was dissolved in deionized water (20 mL) and the solution was passed through a Dowex 50 × 8 (H^+) column. Upon freeze-drying of the eluate, the product was then freeze-dried to yield a pale brown solid **7** (270 mg, 90%).

Polymerization of NIPAM Initiated with Compound [7]. Photopolymerization initiated using compound **7** was performed in an aqueous solution of NIPAM under a nitrogen atmosphere with UV irradiation (light intensity, 0.5 mW/cm^2) using a 250 W Hg lamp (SPOT CURE, USHIO, Tokyo, Japan). After polymerization, the reaction mixture was dialyzed followed by freeze-drying to yield a white or pale brown solid (PNIPAM–heparin [8]).

Fluorescence-Labeled PNIPAM–Heparin. Fluorescence-labeled PNIPAM–heparins were prepared by condensation reaction with 5-(4,6-dichlorotriazin-2-yl)aminofluorescein (DTAF, Sigma) according to our method previously reported[12] (the number of fluorescent dye molecules conjugated to heparin ranged from 2 to 5 per molecule).

Transmittance Measurement. The LCST of PNIPAM–heparin was determined by measuring the optical transmittance at 600 nm of an aqueous PNIPAM–heparin solution (0.5 wt %) at a heating rate of 0.5 °C/min from 25 to 40 °C. The temperature at onset of decrease in transmittance, which was determined with an accuracy of 0.1 °C by a thermosensor that was directly immersed into a solution, was defined as the LCST.

Adsorption and Desorption. The PNIPAM–heparin-coated PET film was prepared as follows. An aqueous solution of PNIPAM–heparin [8] (0.5 wt %, 5 μL) was placed on the surface of a circular PET film (diameter, 15 mm), and the film was dried at 20 °C. The film surface was rinsed with either cold water (20 °C) or hot water (40 °C). Alternatively, PNIPAM–heparin-adsorbed PET film was prepared by immersion in a 0.5 wt % aqueous solution of PNIPAM–heparin [8] (PNIPAM mol wt = 1×10^4) at 20 °C. Then, the film was immersed in a solution at either 20 or 40 °C for 3 h. Then, the film surface was rinsed with either cold water (20 °C) or hot water (40 °C).

Adsorbed PNIPAM–Heparin. The amounts of adsorbed PNIPAM–heparin on surfaces were determined by measurement of average fluorescence intensity of fluorescence-labeled PNIPAM–heparin-coated surfaces under a confocal laser scanning microscope (CLSM) using the standard linear relationships between the fluorescence intensity and the amount of fluorescence-labeled PNIPAM–heparins.

Antithrombin III Trapping. The PNIPAM–heparin-treated film surface was treated with 1% BSA in phosphate-buffered solution (PBS) for 30 min to block nonspecific adsorption of ATIII or antibodies and then immersed in the ATIII-containing PBS (1 unit/mL) for 30 min at 4 °C. Then, the films were thoroughly washed with a buffer solution for fluorescence staining. The

(15) Sugiura, N.; Sakurai, K.; Karasawa, K.; Sakurai, S.; Kimata, K. J. *Biol. Chem.* **1993**, *268*, 15779–15787.

Scheme 1. Reactions for Synthesis of PNIPAM–Heparin

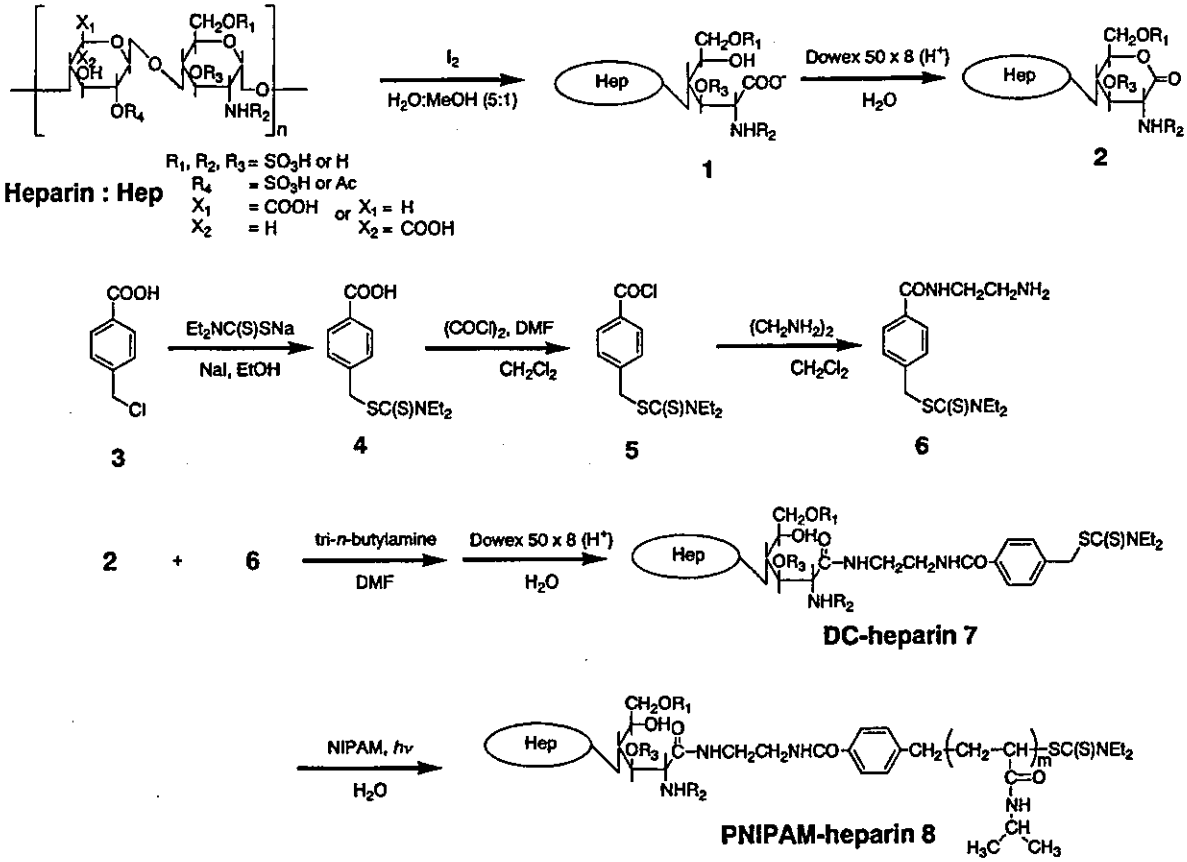

PNIPAM–heparin–ATIII complex coated film surfaces were treated by an enzyme-labeled-antibody technique using an ABC kit (Vector Laboratories, Inc., Burlingame, CA) and visualized under the CLSM. The treated films were incubated in the medium DMEM (Dulkecco's modified Eagle's medium; Gibco, Grand Island, NY) containing 10% fetal bovine serum (FBS, Life Technologies, USA) to see whether PNIPAM–heparin is stably anchored on the surface in a body-simulated fluid. Staining was performed according to the manufacturer's instruction. Briefly, the first step involves treatment with a buffer solution containing a sheep monoclonal antibody. Then, a buffer solution containing a biotinylated secondary antibody was applied; an avidin solution and a biotinylated alkaline phosphatase (AP) solution were subsequently applied to the film surface. An AP substrate was used for chromogenic staining. The colorimetric enzyme–substrate reaction allows visualization of fixed proteins only. The film surfaces were imaged using the CLSM. The ABC–AP substrate conjugated maximum excitation closely matches the 543-nm spectral line of the argon-ion laser, making it the fluorochrome of choice for the CLSM.

Results

Preparation of PNIPAM-Grafted Heparin [8]. Heparin, terminally grafted with PNIPAM, was prepared by sequential reactions involving oxidation cleavage (compound **1**, Scheme 1), lactone ring formation (compound **2**), and dithiocarbamylation (compound **7**) at the terminal sugar moiety and subsequent photopolymerization, which was initiated from the dithiocarbamate (DC) group at the terminus of heparin, producing PNIPAM-grafted heparin (PNIPAM–heparin; compound **8**). The former two steps were carried out following a previously reported method using iodine-induced cleavage and subsequent proton-catalyzed cyclization.[15] This method has been proven to cause minimal damage to both backbone and side chains of polysaccharides.[15] Dithiocarbamylation was conducted by a ring-opening reaction of lactone-terminated heparin [2] with DC-derivatized ethylenediamine (compound **6**), which was prepared using 4-chloromethyl benzoic acid (compound **3**) as a starting material. UV irradiation of an aqueous solution containing DC-derivatized heparin [7] in the presence of NIPAM resulted in successive photopolymerization initiated from the terminus of the heparin molecule in a living polymerization fashion, which was deduced from previous papers.[16,17]

To estimate the molecular weight of the PNIPAM graft chain, we utilized our recently reported reaction condition–molecular weight relationship, which was established using the iniferter poly(ethylene glycol) having a DC group at one end and a methyl group at the other end (DC–PEG).[21] In the present experiments, the reaction condition (photointensity, 0.5 m W/cm^2; photoirradiation time, 30 min) was the same as that previously reported. On the basis of this reaction condition–molecular weight relationship, we assumed that the estimated number-average molecular weights of the PNIPAM graft chains of heparin, thus prepared, ranged from approximately 2×10^3 to 1×10^5 g/mol and the polydispersity index was approximately 1.2–1.3, which depends on the DC and NIPAM concentrations (Table 1). An increase in NIPAM concentration and a decrease in the DC–heparin concentration resulted in higher-mol-wt PNIPAM grafted at the terminal end of heparin.

The resultant PNIPAM–heparin [8] was a white solid and dissolved in water at room temperature but precipi-

(16) Nakayama, Y.; Matsuda, T. *Macromolecules* **1999**, *32*, 5405.
(17) Lee, H. J.; Nakayama, Y.; Matsuda, T. *Macromolecules* **1999**, *32*, 6989.

Table 1. Estimated Mol Wt of PNIPAM–Heparin Prepared at Different Molar Concentrations of Iniferter and Monomer and Thermoresponsive Properties

sample	DC–heparin[a] [mmol/L]	NIPAM [mmol/L]	mol wt of PNIPAM chain[b] ($\times 10^4$ g/mol)	LCST[c] (°C)	equilibrium transmittance (%)
a	0.50	10	0.2	37.1 ± 0.4	49
b	0.50	10	0.5	35.1 ± 0.3	85
c	0.01	10	1.0	34.6 ± 0.1	100
d	0.01	50	5.0	34.0 ± 0.1	100
e	0.01	100	10.0	34.0 ± 0.1	100

[a] Iniferter-derivatized dithiocarbamyl heparin (compound **7** in Scheme 1). [b] Estimated from polymerization behavior using dithiocarbamyl poly(ethylene glycol), DC–PEG, under the same conditions described in our previous paper. [c] Lower critical solution temperature at 0.5% concentration.

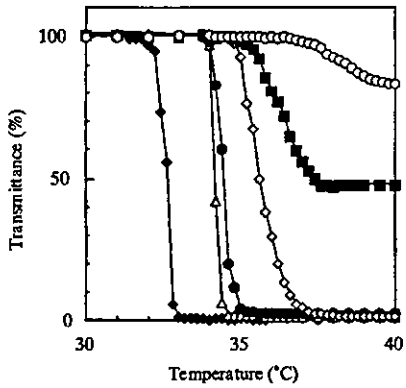

Figure 1. Thermoresponsive change in transmittance of PNIPAM–heparin with PNIPAM of different mol wt's in aqueous solution. The mol wt of PNIPAM in PNIPAM–heparin: 2×10^3 (○), 5×10^4 (■), 1×10^4 (◇), 5×10^4 (●), and 1×10^5 (△); PNIPAM homopolymer (◆). Concentration of PNIPAM–heparin: 1 wt %. Heating rate: 0.5 °C/min.

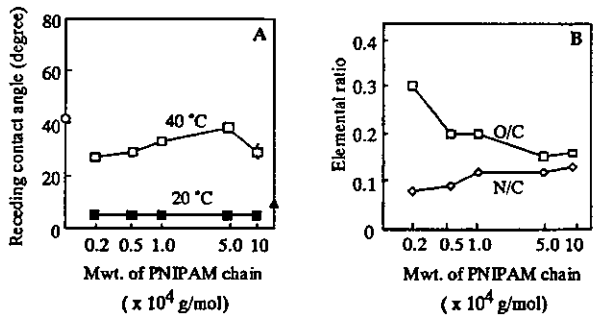

Figure 2. (A) Receding contact angles of PNIPAM–heparin-coated surfaces washed with water at 20 °C (□) or 40 °C (■). (A) Nontreated PET film (○) and PNIPAM homopolymer (▲). (B) Elemental ratios measured by XPS of the PNIPAM–heparin-coated surface: O/C (□) and N/C (●). The film surfaces were washed with water at 40 °C. Theoretical elemental ratios of sodium heparin salt were as follows: O/C, 0.65; N/C, 0.04; S/C, 0.12. Theoretical values of PNIPAM homopolymer were as follows: O/C, 0.17; N/C, 0.17.

tated in the physiological temperature range. Figure 1 shows the thermoresponsive change in transmittance of PNIPAM–heparin in 1% aqueous solution. The PNIPAM homopolymer (mol wt = 2×10^5 g/mol), which was prepared by radical polymerization in a previous study, exhibited a very sharp drop in transmittance at approximately 31.9 ± 0.1 °C and completely precipitated above this temperature. Table 1 also lists the LCST of PNIPAM–heparins with different mol wt graft chains. For PNIPAM–heparins with higher-mol-wt PNIPAM (PNIPAM mol wt = 5×10^4 and 1×10^5 g/mol), a sharp drop in transmittance and LCST of approximately 34.0 ± 0.1 °C were noted. For PNIPAM–heparins with lower-mol-wt PNIPAM, a gradual increase in LCST, a temperature-dependent drop in transmittance, and a high equilibrium transmittance were noted. LCST is gradually increased as the molecular weight of the PNIPAM graft chain is decreased. For example, PNIPAM–heparin with the PNIPAM mol wt of 1×10^4 g/mol exhibited complete precipitation at 34.6 ± 0.1 °C, whereas PNIPAM–heparin with a lower-mol-wt PNIPAM exhibited incomplete precipitation (equilibrium transmittance and LCST were approximately 85% and 35.1 ± 0.3 °C, respectively, for PNIPAM with the mol wt of 5×10^3 g/mol and approximately 49% and 37.1 ± 0.4 °C for that with the mol wt of 2×10^3 g/mol, respectively).

Thermoresponsive Adsorption/Desorption Characteristics on PET. The PET samples were coated with a 0.5 wt % aqueous solution of PNIPAM–heparin [8] and subsequently air-dried and subjected to washing with water at either 20 or 40 °C. The mol wt dependency for PNIPAM–heparin [8] of wettability and surface composition is shown in Figure 2. Irrespective of the mol wt of PNIPAM, the receding contact angle for samples washed with water at 40 °C was less than 10°, which is almost the same as that of the PNIPAM homopolymer (12°) (Figure 2A). On the other hand, the receding contact angle for samples washed with water at 20 °C was quite high, 30–40°, which is lower than that of the homopolymer (49.2°) but close to that of the noncoated PET film. XPS measurement (determined at the takeoff angle of 90 °C) of samples washed with water at 40 °C showed that an increase in the mol wt of PNIPAM increased N/C and decreased O/C, both of which approached the theoretical values of the PNIPAM homopolymer (0.17 for each) (Figure 2B). Figure 3 shows high-resolution C_{1S} and O_{1S} XPS spectra obtained for PNIPAM–heparin with the highest mol wt graft chain (1×10^5 g/mol) (Figure 3B). Upon washing at 40 °C, subpopulations of C_{1S} and O_{1S} were quite apart from those of the nontreated PET films: for the C_{1S} subpopulation, the carbonyl carbon peak at 289.0 eV relative to the C–N or C–O peak at 286.7 eV (note that hydrocarbon carbon is standardized at 285.0 eV) became larger, and for the O_{1S} subpopulation, the carbonyl oxygen peak (532.7 eV) relative to the ether or hydroxy oxygen peak (534.3 eV) also became larger, whereas upon washing at 20 °C, these relative peak intensities tended to decrease but were still larger than that of nontreated PET film. Since the carbonyl group is mainly derived from the PNIPAM molecule, these results strongly indicate that PNIPAM–heparin with a high mol wt graft chain covered the outermost surface of the adsorbed layer on PET at 40 °C, but some fraction of adsorbed PNIPAM–heparin apparently desorbed upon washing at 20 °C. This temperature dependence of adsorption/desorption was more markedly observed for PNIPAM–heparin with the lowest mol wt of PNIPAM. From C_{1S} and O_{1S} spectral analysis, a low extent of adsorption at 40 °C and a high extent of desorption at 20 °C were clearly noticed (Figure 3A).